BBC RD 1977/25

BBC

1974
THE QUEEN'S AWARD TO INDUSTRY

RESEARCH DEPARTMENT

REPORT

Ground-wave propagation at medium frequency in built-up area

J.H. Causebrook, Ph.D., B.Sc., C.Eng., M.I.E.E.

Research Department, Engineering Division
THE BRITISH BROADCASTING CORPORATION July 1977

BBC RD 1977/25
UDC 621.391.81:
621.3.029.53

GROUND-WAVE PROPAGATION AT MEDIUM FREQUENCY IN BUILT-UP AREAS

J.H. Causebrook, Ph.D., B.Sc., C.Eng., M.I.E.E.

Summary

Work has been carried out to seek a better understanding of the way m.f. ground-wave field strengths are influenced by buildings. Measurements were made which showed that, in and near built-up areas, the field strength distance relationship is often different from that expected on the basis of conventional theories. The theory of propagation has been extended and applied to explain the results. The end product is a computer calculation system for typical situations.

Issued under the authority of

G.D. Monteath

Head of Research Department

Research Department, Engineering Division,
BRITISH BROADCASTING CORPORATION

July 1977

(RA-163)

GROUND-WAVE PROPAGATION AT MEDIUM FREQUENCY IN BUILT-UP AREAS

GROUND-WAVE PROPAGATION AT MEDIUM FREQUENCY IN BUILT-UP AREAS

J.H. Causebrook, Ph.D., B.Sc., C.Eng., M.I.E.E.

1. Introduction

For more than 50 years concern has been expressed about the loss of field strength experienced in built-up areas at m.f. The concern has been increased lately in the U.K. as a result of the poor fields received from local broadcast transmitters in cities, from transmitter sites on the outskirts. A study has therefore been made with the objectives of understanding the nature of this loss, and producing a method of predicting its extent.

It is well known that higher frequencies in the m.f. band have smaller ground-wave field strengths for a given transmitter radiated power, but it was suspected that in towns the difference was greater than conventional theories would predict. Many m.f. field strength measurements have been taken over the years but they were not considered adequate for the present analysis. This was because they were mostly taken to determine the extent of service areas and did not provide a continuous series of field measurements from close to the transmitter to beyond the town to be served.

Thus the first part of the project consisted of a measurement campaign. The results confirmed that losses at higher frequencies exceeded the values expected from existing theory and further inconsistencies were found. The second part of the work consisted of a theoretical study, and an extension of the theory of ground-wave propagation was developed which could cover the practical situation of built-up environments.

The general form of the extended theory was written as a computer program with certain weighting factors left undefined. These factors were adjusted by an optimization procedure within the program so that a satisfactory fit to the measurements was achieved. The resulting values for the weighting factors indicated some imperfections in the theory. A method of overcoming these is suggested in this report, but the detail of this is left for future work.

The final part of the project was to write another computer program which can be used for prediction work. This program not only uses the new theory to allow for the built-up environment but also an integral equation method of calculation which is more satisfactory for profiles which are irregular and inhomogeneous. The comparisons between the results of this program and the measurements taken are good.

2. The measurement campaign

The measurement campaign was concentrated along two radial lines from the Brookmans Park transmitter (29 km to the north of central London), both passing through the London area. These were on bearings of 181 and 169 degrees east of grid North, extending to about 50 km from the transmitter. Routes for the measuring vehicle were chosen which ran as close to the radial lines as possible. The measurements were made on three frequencies: 908, 1214 and 1457 kHz, these being the BBC programmes Radio 4, Radio 1 and Radio London respectively.

The measurements were made with equipment which was based upon that described in Reference 1. However, modifications and additions were incorporated to produce a more satisfactory arrangement for the particular task. Firstly, a pen recorder was incorporated so that a record could be obtained which had a chart displacement proportional to distance travelled (using pulses from the vehicle speedometer). Secondly, the original receiver was unsatisfactory because of non-linearity and instability of gain and frequency response, so it was replaced by a better instrument. Thirdly, the original equipment was meant to take readings while the vehicle was stationary, so it was necessary to overcome the directional property of the loop aerial by manually keeping it on bearing.

The chart recordings were highly variable, mainly due to multipath propagation. To obtain a more convenient set of results the charts were analysed in sections, equivalent to 500 metres along the radial line. From this analysis median values of magnetic field strength, H, were obtained. It is usual to quote results in electric field strengths, E, but the conversion in this case would depend upon an unknown space impedance. It was therefore preferred to retain the signal strength measurement in terms of H in amperes per metre. The analysed values were plotted on graphs of 20 $\log_{10}(Hd)_{mA}$ against distance, d_{km}. These graphs are reproduced in Figs. 1 and 2.

The interesting feature of these plots is that, in the first section, the fields are higher than expected and then a steep drop occurs to be followed by an increase beyond the densely built-up area. An extra feature should be noted on the 169° radial, which is a further reduction associated with the tall buildings in Croydon. It will also be noted that the steep drop does not occur at the same distance for each frequency. For 908 kHz it is approximately at 30 km from the transmitter and for 1457 kHz it is at 20 km; the distance of this reduction for 1214 kHz lies between these values.

In addition to the van measurements some values were obtained away from the vehicle using the internal aerial and calibration system in the receiver. These were taken at distances from the transmitter of between 400 and 2500 metres. They are plotted on Fig. 3. The purpose of these measurements was to obtain results which were not restricted to roads. Thus they could be taken in areas as free of man made objects as possible and the radial line could be followed more closely. In this way a determin-

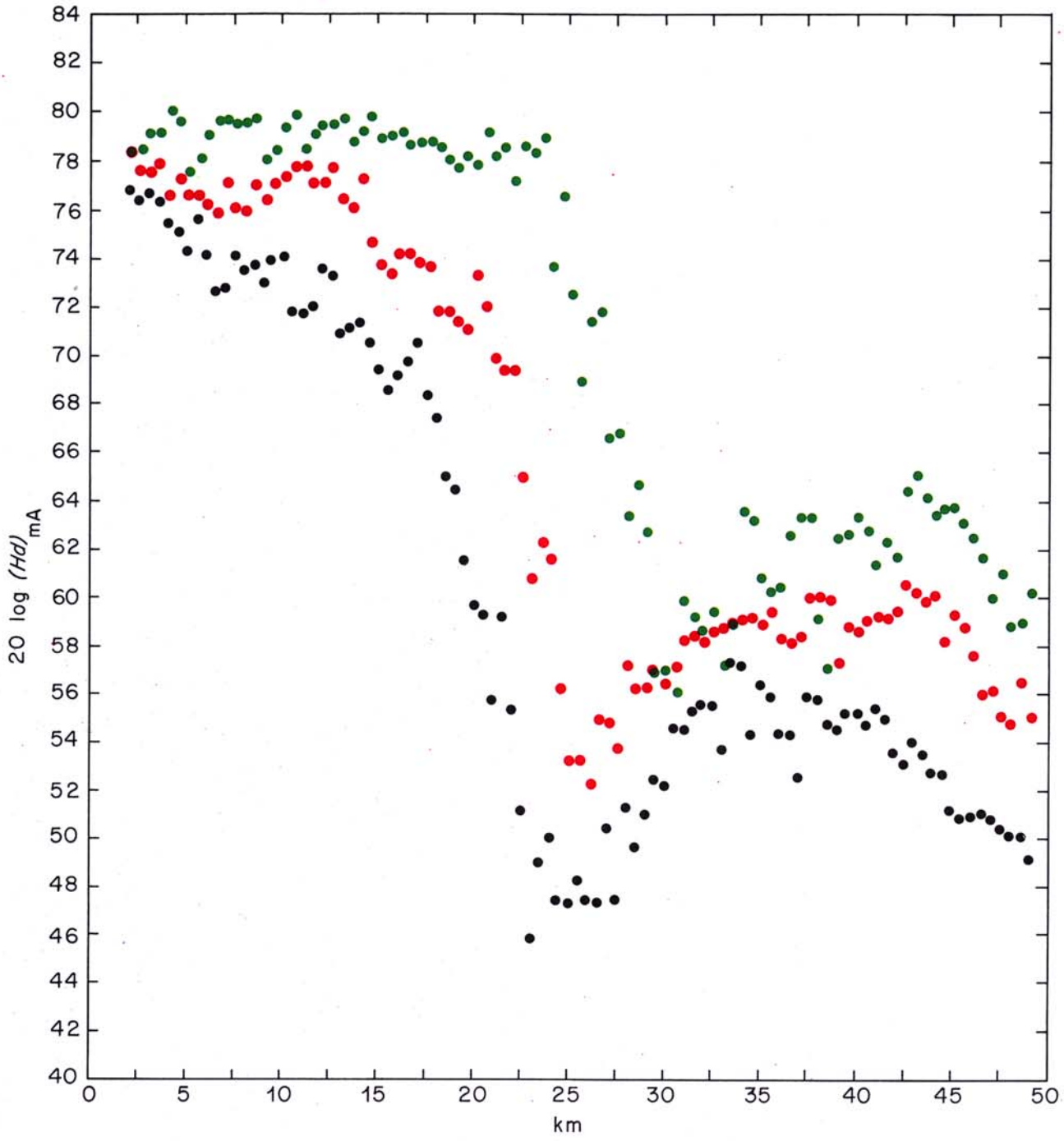

Fig. 1 - Road measurements made along the radial 181° E.G.N. (three frequencies)

● 908 kHz ● 1214 kHz ● 1457 kHz

ation of the point where the graphs of 20 $\log_{10}(Hd)$ should intersect the zero-distance axis will be known to higher accuracy. Thus in later graphs, Figs. 8 to 13, we are able to match calculations and measurements.

3. Theory

The existing calculation methods depend upon the assignment of values to ground conductivity, σ, and, less significantly, relative permittivity, ϵ. Then the Sommerfeld theory gives a method for prediction of field strength over a homogeneous smooth earth. A description of such a calculation is given in Reference 2, and from this method a set of curves can be drawn for simple predictions.[3] If there is a limited change of ground constants along the path then a prediction could be made by the Millington method.[4]

For towns it has been the practice to assign an effective conductivity value. This procedure was tried in an attempt to reproduce the measurements mentioned in the previous section, but the results were poor. Thus the possibility of producing more satisfactory methods was explored.

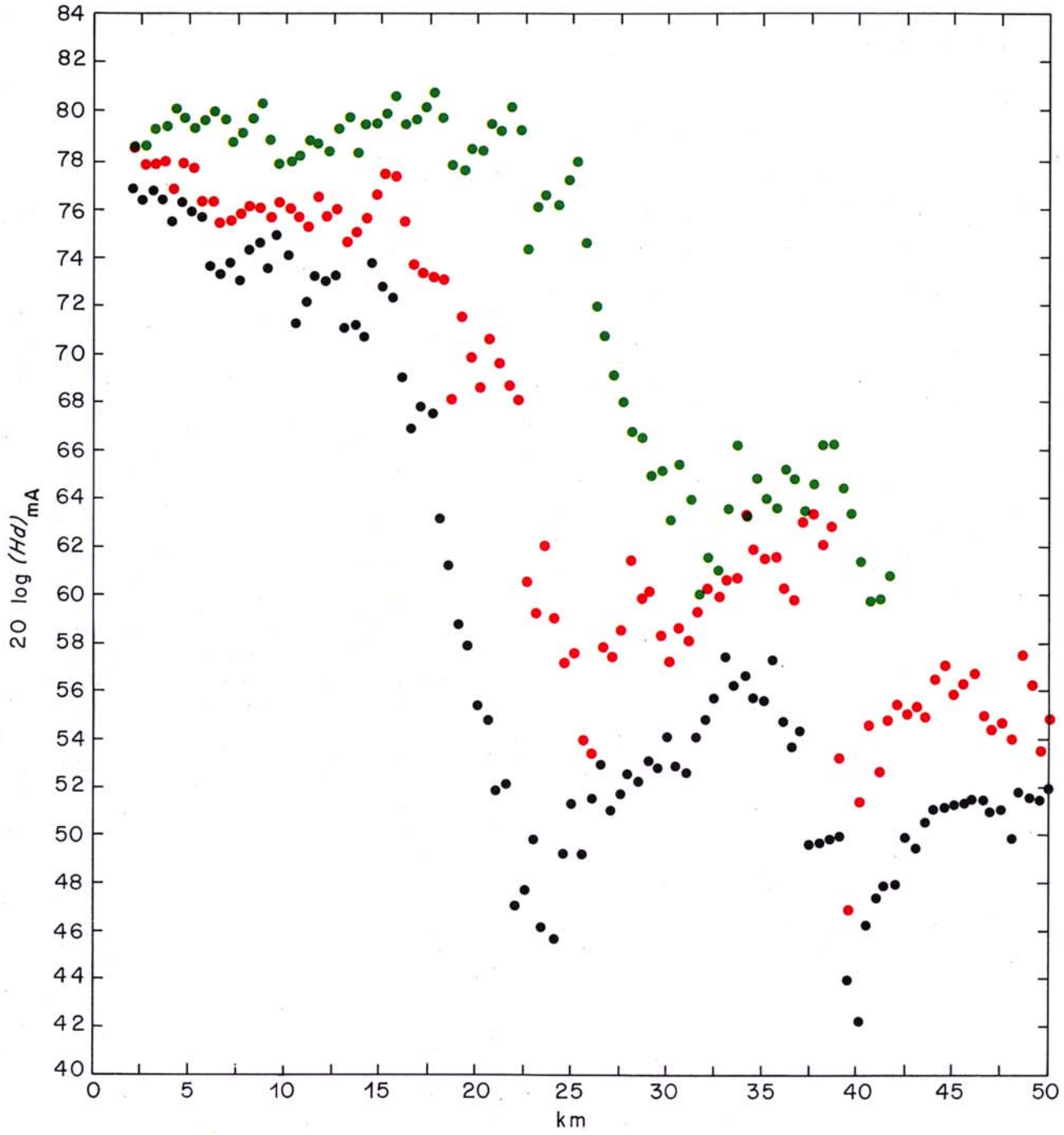

Fig. 2 - Road measurements made along the radial 169° E.G.N. (three frequencies)

● 908 kHz ● 1214 kHz ● 1457 kHz

Hufford[5] gives an integral equation which permits calculation of field strength over smoothly varying inhomogeneous terrain. The ground-wave attenuation factor $g(R)$ at distance R relative to a perfectly conducting plane earth is determined in this method by the equation:

$$g(R) = 1 - \sqrt{\frac{j}{\lambda}} \int_0^R (\eta + \psi)\, e^{-j\beta\xi}\, g(r) \sqrt{\frac{R}{r(R-r)}}\, dr \quad (1)$$

where $\beta = \frac{2\pi}{\lambda}$ (λ = wavelength)

ψ = angle (in radians) between the line from the receiver to the surface at range r and the tangent to the surface, at this point.

ξ = distance between terminals* subtracted from the sum of distances from terminals to the surface at r (see Fig. 5, Section 4).

η = relative surface impedance at r.

* The word terminals refers to the transmitter and the receiver at point R.

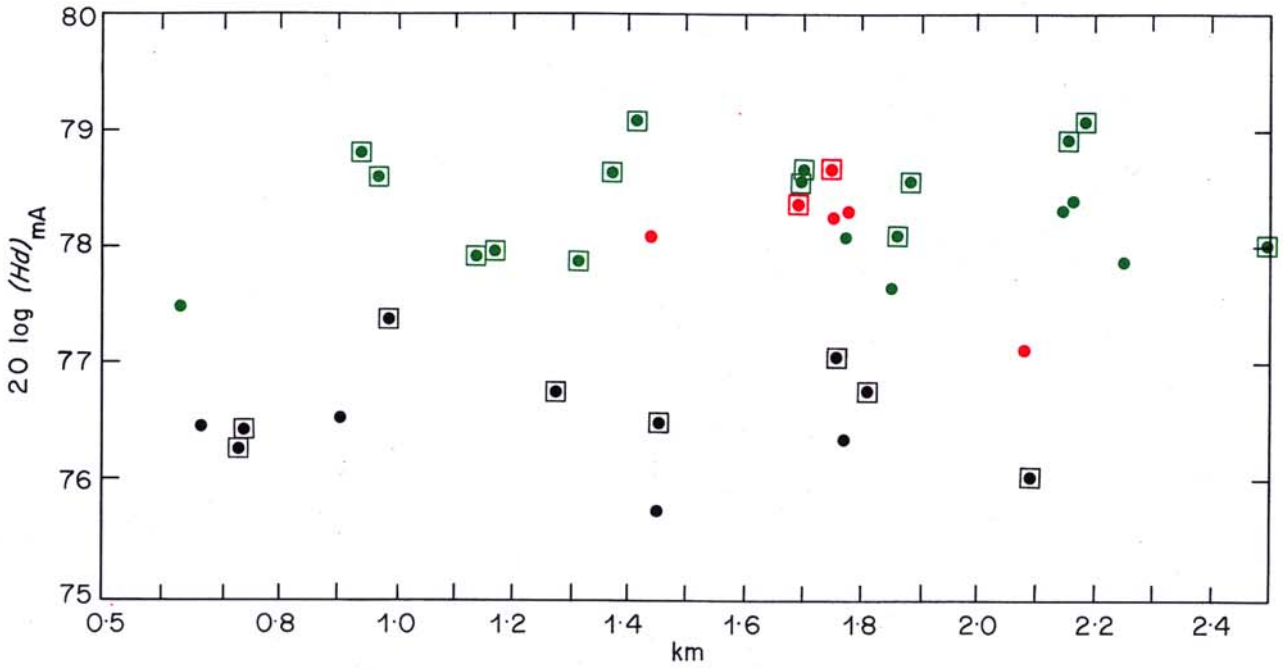

	Radial bearing	
Freq. kHz	181°	169°
908	●	◉
1214	●	◉
1457	●	◉

Fig. 3 - Measurements away from the vehicle

For an uncluttered surface and a plane wave incident at an angle θ to the normal to the surface we have:

$$\eta = \frac{[\epsilon - j60\sigma\lambda - \sin^2\theta]^{\frac{1}{2}}}{\epsilon - j60\sigma\lambda} \qquad (2)$$

In a built-up area it will be as if another medium were placed between the ground and the 'free-space' above. Thus we require a modified value of η appropriate to these conditions. If we were to think of this modified value as resulting from an 'effective' conductivity we would be restricted to a value of η which has roughly equal real and imaginary parts. An initial attempt to match the measurements this way indicated that what was required was a value of η which had a much larger positive imaginary part. The reasons for this can be appreciated from an examination of the Appendix (Section 10).

The two sections that follow give a theoretical plausibility to the proposal to adopt a modified value of η as suggested by the empirical work. The analyses give an indication as to the form and magnitude of η that is appropriate to built-up areas. Exact values cannot be expected from these analyses as:

1. The building layer is treated as if it can be described by a macroscopic theory, but in practice the sizes of structures are not insignificant compared to a wavelength.

2. Only a single plane wave is considered.

3. The method does not consider signals arriving by scattering (multipath) from points other than those on the line between transmitter and receiver.

3.1. Low building density theory*

At l.f. and m.f. many man made structures (lamp posts, steel framing, house-wiring and plumbing) may be considered as earthed parasitic unipoles. Thus an incident electric field induces a current in these structures. To analyse the effect of this we will use a co-ordinate system and geometry as shown in Fig. 4. It is possible to assume a current density in the vertical direction given by:

$$I(z) = j\frac{\beta}{\eta_o} K(z) E_z \qquad (3)$$

where η_o is the intrinsic impedance of free space and $K(z)$ is a value decreasing with height and dependent on the length of the unipole and its characteristic impedance.

From Maxwell's equations in the building layer:

$$-\frac{\partial H_x}{\partial y} = j\frac{\beta}{\eta_o}[1 + K(z)]\ E_z \qquad (4)$$

If a plane wave exists in the space above this layer the component of the propagation coefficient in the y direction

* The original idea for this approach was suggested by P. Knight.

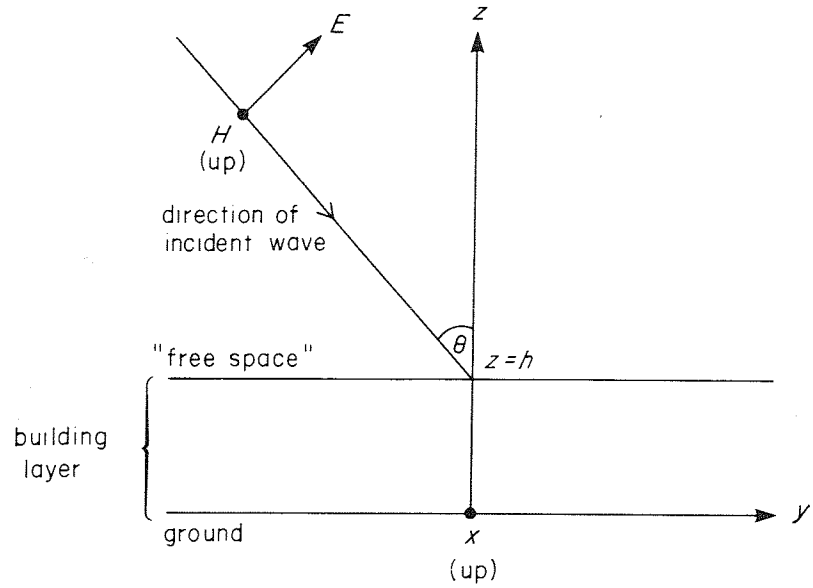

Fig. 4 - Co-ordinate system and geometry of the model

(see Fig. 4) is $-j\beta \sin\theta$ in all the media (free space, building layer and the ground).

Now let us consider a small stratum in the building layer, between the heights $z = t$ and $z = t + \delta t$, in which we consider the vertical propagation coefficient as constant at $\gamma(t)$ denoted as Γ and $K(z)$ constant having the value $K(t)$ denoted as K'. At t there will be downgoing and upgoing waves characterized by H_d and H_u. Thus in this stratum:

$$H_x = \left[H_d\, e^{\Gamma(z-t)} + H_u\, e^{-\Gamma(z-t)}\right] e^{-j\beta y \sin\theta} \qquad (5)$$

The corresponding electric field components will be:

$$E_y = \frac{\eta_o}{j\beta}\frac{\partial H_x}{\partial z} = \frac{\eta_o \Gamma}{j\beta}\left[H_d e^{\Gamma(z-t)} - H_u e^{-\Gamma(z-t)}\right] e^{-j\beta y \sin\theta} \qquad (6)$$

$$E_z = \frac{j\eta_o}{\beta(1+K')}\frac{\partial H_x}{\partial y} = \frac{\eta_o \sin\theta}{1+K'} H_x \qquad (7)$$

Also from Maxwell's equations:

$$H_x = \frac{j}{\beta\eta_o}\left(\frac{\partial E_z}{\partial y} - \frac{\partial E_y}{\partial z}\right) = \left(\frac{\sin^2\theta}{1+K'} - \frac{\Gamma^2}{\beta^2}\right) H_x \qquad (8)$$

Therefore:

$$\Gamma = j\beta\left(1 - \frac{\sin^2\theta}{1+K'}\right)^{1/2} \qquad (9)$$

Subject to certain criteria it is valid to accept the definition of relative surface impedance as being given by:

$$\eta(t) = \frac{1}{\eta_o}\left(\frac{E_y}{H_x}\right)_{z=t} \qquad (10)$$

Therefore from Equations (5) and (6) at $z = t$:

$$\eta(t) = \frac{\Gamma}{j\beta}\frac{H_d - H_u}{H_d + H_u} \qquad (11)$$

and at $z = t + \delta t$:

$$\eta(t+\delta t) = \frac{\Gamma}{j\beta}\frac{H_d e^{\Gamma\delta t} - H_u e^{-\Gamma\delta t}}{H_d e^{\Gamma\delta t} + H_u e^{-\Gamma\delta t}} \qquad (12)$$

Approximating for $e^{\pm\Gamma\delta t}$ and from Equations (11) and (12) we get:

$$\eta(t+\delta t) = \frac{\eta(t) + \frac{\Gamma^2}{j\beta}\delta t}{1 + j\eta(t)\beta\delta t} \qquad (13)$$

Because both $\eta(t)$ and $\beta\delta t$ are small this may be further approximated to give:

$$\eta(t+\delta t) = \eta(t) + j\beta\left(1 - \frac{\sin^2\theta}{1+K'}\right)\delta t \qquad (14)$$

where we have also substituted for Γ using Equation (9).

If we consider the depth of the stratum reducing to an infinitesimal and we integrate from ground level to the top of the building layer we get:

$$\int_{\eta(o)}^{\eta(h)} d\eta = j\beta \int_o^h \left(1 - \frac{\sin^2\theta}{1+K(t)}\right) dt \qquad (15)$$

Therefore

$$\eta(h) = \eta(o) + j\beta\left[h - \sin^2\theta \int_o^h \frac{dt}{1+K(t)}\right] \quad (16)$$

In the present problem we wish to consider waves at near grazing angle. To simply put θ to 90° throughout the above analysis would introduce some awkward zeros. Thus θ must be considered as only approaching 90°.

To solve the integration in Equation (16) it is necessary to assume the form that K should take. There are many factors which contribute to a discussion about the best form for this variable, such as the dimensions of the re-radiating objects and the fact that a given area will have a mixture of these. For the present purposes a triangular height distribution is a reasonable compromise. Thus:

$$K(t) = \frac{nh^2\eta_o}{2\eta_c}\left(1 - \frac{t}{h}\right) \quad (17)$$

Where n = the number of structures per unit area and
η_c = the characteristic impedance of the unipoles.

The predominant objects in the less built-up areas are two-storey houses and lamp-post like structures. They both have similar heights but there are more houses in most areas. With the use of Reference 6 we get η_c approximately equal to 20 ohms for houses, and 200 ohms for lamp-posts. Thus the houses will dominate the value of K. It is now possible to assume that houses are roughly cubic in shape so that nh^2 equals the fraction of area covered by houses, B say. Thus Equation (16) becomes:

$$\eta(h) = \eta(o) + j\beta h\left[1 - \frac{\log_e(1+10B)}{10B}\right] \quad (18)$$

3.2. High building density theory

The analysis of Section 3.1 becomes progressively less valid as the building density becomes large. This is for several reasons, but the most important is that the impedance of the tops of buildings is neglected. To determine the type of formulation required in the highly built-up areas consider grooves cut into a highly conductive surface and exposing poorer conductivity at the base. In this case we may distinguish areas giving three different surface impedance:

1. Roof tops where we will assume $\eta(h)$ equals zero
2. Streets parallel to the line of propagation where $\eta(h)$ equals $\eta(o)$
3. Streets at right-angles to the propagation direction. Here $\eta(h)$ may be obtained by analogy to a transmission line. From Jordan,[2] Chapter 8, we obtain:

$$\eta(h) = \frac{\eta(o) + j\tan\beta h}{1 + j\eta(o)\tan\beta h} \quad (19)$$

Provided $\beta h < \pi/4$, only a small error is introduced if we make a similar approximation to that which gave Equation (14).

Then

$$\eta(h) = \eta(o) + j\beta h \quad (20)$$

It is not practicable to use these values individually in the calculation system. A compromise surface impedance may be obtained by taking a weighted average of roof tops and the two directions of streets. Thus as B is the fraction of area covered by buildings we may assume that each type of street covers an area $\frac{1}{2}(1-B)$, which leads to:

$$\eta(h) = (1-B)\,\eta(o) + \frac{1-B}{2}\,j\beta h \quad (21)$$

3.3. A combined result

It is now convenient to combine the results given by Equations (18) and (21). However, before doing this it should be pointed out that $\eta(o)$ will not necessarily remain at the value which would have existed before the area was built-up. Let us refer to this indiginous surface impedance as η_i. It is then possible to denote the combined result thus:

$$\eta = f_1(B)\,\eta_i + f_2(B)\,j\beta h \quad (22)$$

where $f_1(B)$ and $f_2(B)$ are functions of building density. The precise form of these functions is not obtainable from theory because building density is not a perfect parameter and the theories are approximate. To overcome this we may determine the functions via the measurements. This may be done with the aid of a computer optimization process, but first it is necessary to decide on the general form of the functions and the constraints which should be placed upon these forms. For example, a non-monotonic situation may be expected because Equation (18) indicates the imaginary part increasing with building density, whereas Equation (21) shows a decrease. An obvious requirement is that the result must tend to η_i when buildings are absent. These considerations led to the following:

$$\left.\begin{aligned} f_1(B) &= (1-B)^{x_1} \\ f_2(B) &= x_2\sqrt{B} + x_3 B + x_4 B^{1.5} \end{aligned}\right\} \quad (23)$$

where the x_i values are to be determined by optimization.

4. The computer calculation system

Before a computer program could be written it was necessary to decide how best to solve an integral of the form given in Equation (1).* Of course, data will be discrete in form, i.e. a quantum of data representing a distance D within a profile. Let the quantum be defined thus:

* The method of solving the integral equation used here is a further development of a method initially proposed by G.D. Monteath.

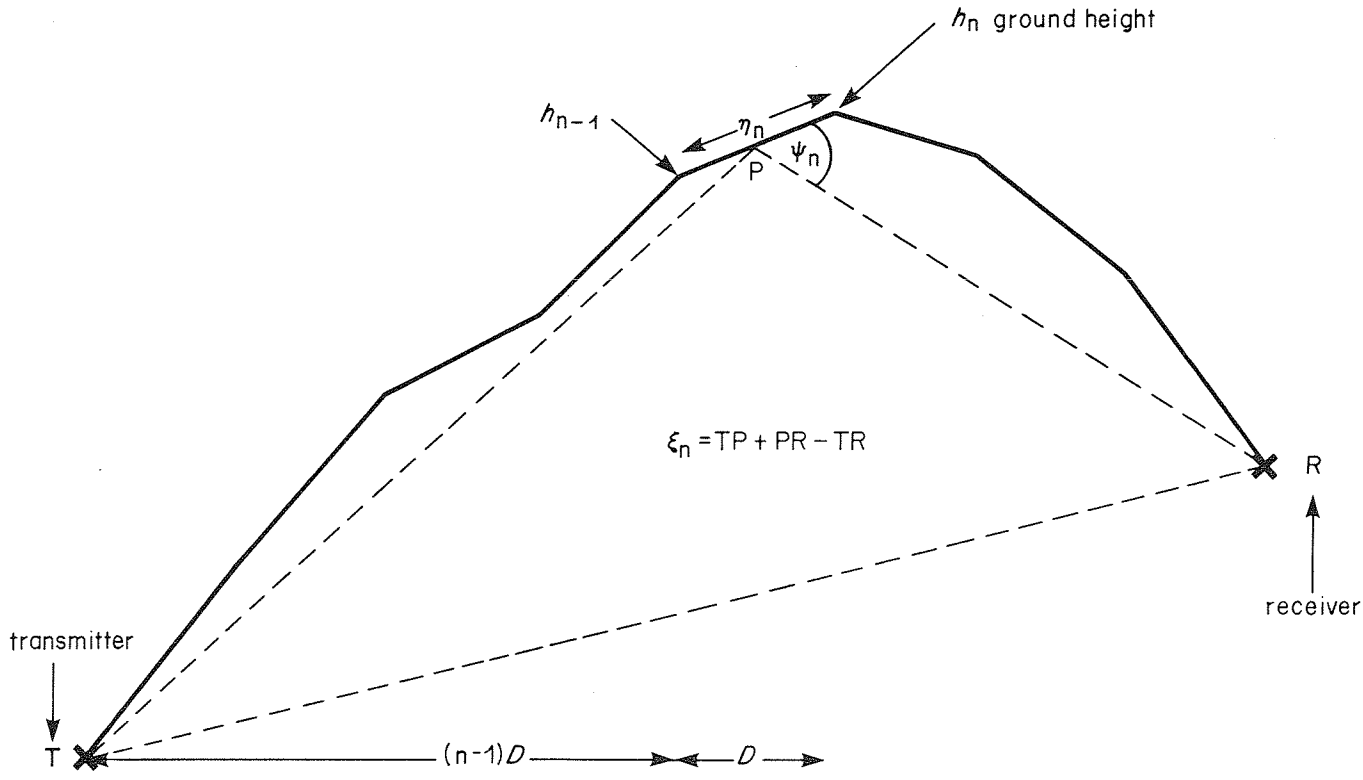

Fig. 5 - Quantized form of the data required for a profile

$$Q_n = (\eta_n + \psi_n)e^{-j\beta\xi_n} \tag{24}$$

where the quantities are defined in Fig. 5.

The essential part of Equation (1) which requires solution now becomes:

$$\sum_{n=1}^{N} Q_n \int_{(n-1)D}^{nD} \frac{g(r)\ dr}{\sqrt{r(ND-r)}} = \sum_{n=1}^{N} Q_n I_n \tag{25}$$

In most intervals we can assume that g varies linearly with r. However, considering the immediate vicinity of the transmitter, this assumption is invalid in the first interval and is inadequate in the second when there are only two intervals. This limitation is overcome by the fact that the first interval should obey the Sommerfeld/Norton formula

$$g = 1 - j\sqrt{\pi\rho}\, e^{-\rho}\, \mathrm{erfc}(j\sqrt{\rho}) \tag{26}$$

Thus to calculate the value, G_1, of g at the end of the first interval:

$$\rho = -j\frac{D\pi}{\lambda}\eta_1^2 \tag{27}$$

To calculate G_2 it is reasonable to assume:

$$\rho = -j\frac{2D\pi}{\lambda}\eta_1\eta_2 \tag{28}$$

To obtain the value I_1, when N is greater than two, Equation (26) may be expanded as a power series. To obtain satisfactory accuracy in the most critical cases it was found that the series needed to contain the first six terms:

$$g = 1 - j(\pi cr)^{1/2} - 2cr + j(\pi c^3 r^3)^{1/2} + \frac{4(cr)^2}{3} - j(\pi c^5 r^5)^{1/2} \tag{29}$$

where c is a constant within the interval. A value of I_1 may now be produced by analytical means. The assumption of linearity will now give us the remaining integral as:

$$I_n = A_n G_{n-1} + R_n G_n \tag{30}$$

where A_n and R_n may be derived analytically.

Then if:

$$W = \sqrt{\frac{\lambda}{jND}} \tag{31}$$

we get

$$G_N = \frac{W - \sum_{n=1}^{N-1} Q_n I_n - Q_N A_N G_{N-1}}{W + Q_N R_N} \tag{32}$$

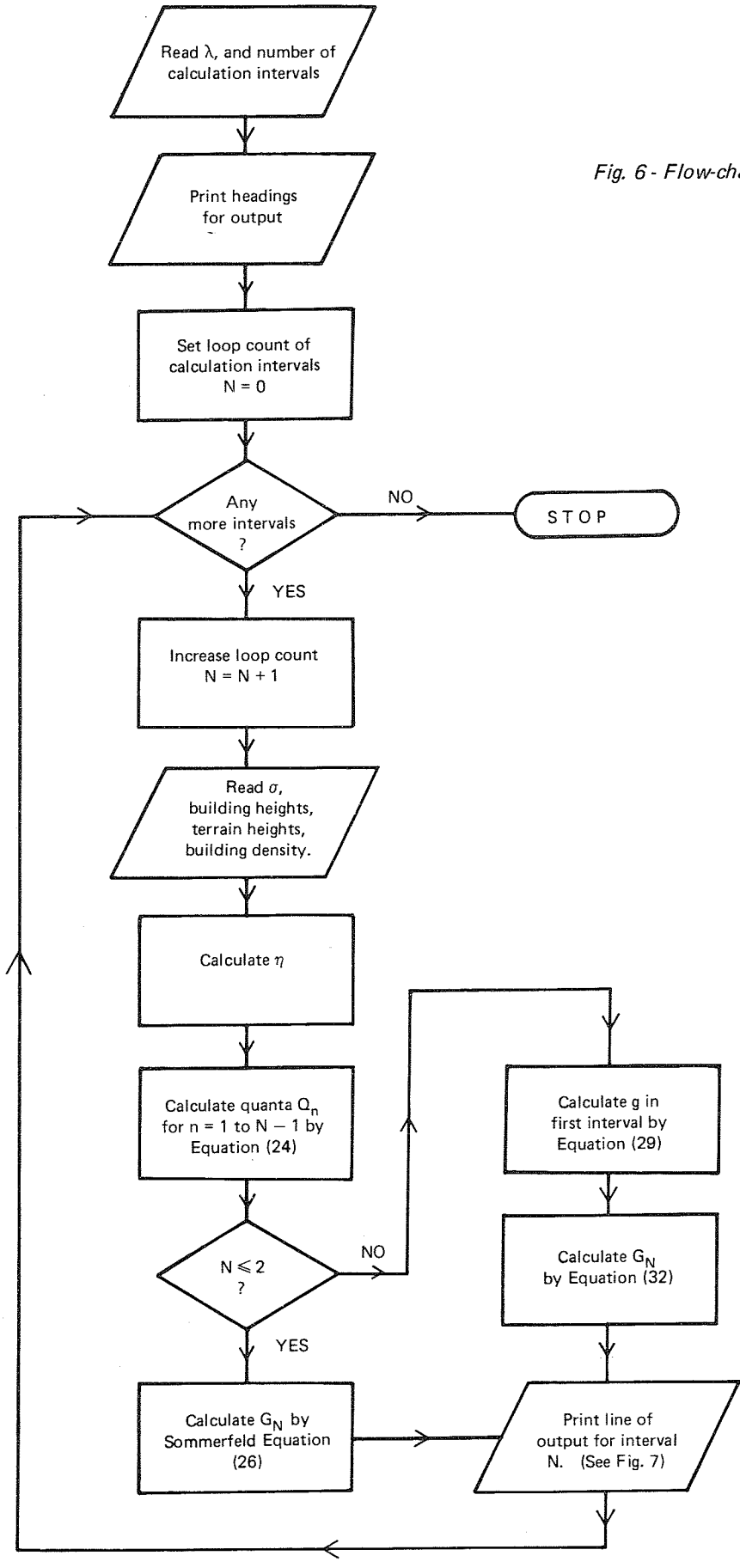

Fig. 6 - Flow-chart of computer program

GROUND-WAVE BY INTEGRAL EQN. INCLUDING BUILDING EFFECTS

LAMBDA(M)= 330

DIST M	HT M	BHT M	F %	SIG MS/M	GN REAL	GN IMAG	...LOSS... MAG	DEG	-DB	E MV/M
500	122	5	11	10	.049	.077	1.064	20	-.5	6747.8
1000	103	5	11	10	.049	.077	1.081	28	-.7	3428.6
1500	105	7	5	10	.050	.080	1.122	33	-1.0	2373.3
2000	113	10	5	10	.050	.092	1.183	39	-1.5	1875.5
2500	125	10	5	10	.050	.092	1.217	44	-1.7	1544.7
3000	114	10	11	10	.049	.105	1.192	54	-1.5	1260.2
3500	113	10	11	10	.049	.105	1.217	59	-1.7	1102.8
4000	123	10	11	10	.049	.105	1.258	62	-2.0	997.4
4500	119	10	11	10	.049	.105	1.230	69	-1.8	867.3
5000	118	10	5	10	.050	.092	1.206	73	-1.6	765.0
5500	115	10	5	10	.050	.092	1.189	77	-1.5	685.7
6000	108	10	5	10	.050	.092	1.166	82	-1.3	616.3
6500	97	10	5	10	.050	.092	1.140	87	-1.1	556.2
7000	100	10	5	10	.050	.092	1.163	88	-1.3	527.2
7500	103	10	5	10	.050	.092	1.163	90	-1.3	491.7
8000	85	10	11	10	.049	.105	1.122	99	-1.0	445.1
8500	61	10	19	10	.047	.113	1.104	107	-.9	412.0
9000	65	10	21	10	.047	.115	1.166	107	-1.3	410.9
9500	64	10	21	10	.047	.115	1.164	111	-1.3	388.8
10000	59	10	21	10	.047	.115	1.150	116	-1.2	364.9
10500	55	10	11	10	.049	.105	1.123	118	-1.0	339.2
11000	60	10	19	10	.047	.113	1.146	120	-1.2	330.6
11500	67	10	19	10	.047	.113	1.148	123	-1.2	316.6
12000	68	10	15	10	.048	.110	1.118	126	-1.0	295.4
12500	69	10	19	10	.047	.113	1.107	130	-.9	280.8
13000	76	10	25	10	.046	.117	1.114	132	-.9	271.8
13500	78	10	25	10	.046	.117	1.093	136	-.8	256.8
14000	82	10	25	10	.046	.117	1.081	139	-.7	244.9
14500	85	10	25	10	.046	.117	1.063	142	-.5	232.6
15000	81	10	25	10	.046	.117	1.030	147	-.3	217.7
15500	66	15	21	10	.047	.148	1.031	157	-.3	211.0
16000	67	15	21	10	.047	.148	1.048	161	-.4	207.7
16500	69	15	21	10	.047	.148	1.039	165	-.3	199.8
17000	73	15	25	10	.046	.152	1.031	170	-.3	192.4
17500	82	15	25	10	.046	.152	1.020	173	-.2	184.8
18000	88	15	21	10	.047	.148	.984	178	.1	173.4
18500	88	15	21	10	.047	.148	.942	184	.5	161.6
19000	90	15	25	10	.046	.152	.918	189	.7	153.3
19500	66	15	39	10	.044	.157	.859	200	1.3	139.8
20000	61	15	44	10	.043	.157	.858	203	1.3	136.1
20500	46	15	39	10	.044	.157	.819	210	1.7	126.8
21000	38	15	39	10	.044	.157	.800	215	1.9	120.8
21500	37	15	44	10	.043	.157	.784	218	2.1	115.7
22000	36	15	44	10	.043	.157	.757	222	2.4	109.1
22500	35	15	44	10	.043	.157	.726	227	2.8	102.4
23000	30	20	44	10	.043	.195	.729	237	2.7	100.5
23500	29	22	44	10	.043	.210	.720	247	2.9	97.2
24000	28	25	44	10	.043	.233	.707	259	3.0	93.4
24500	27	25	44	10	.043	.233	.664	271	3.6	86.0
25000	21	25	44	10	.043	.233	.609	283	4.3	77.3
25500	6	25	44	10	.043	.233	.550	297	5.2	68.4
26000	6	25	44	10	.043	.233	.501	306	6.0	61.2

Fig. 7 - Output of computer program

5. The computer optimization process

The field calculations can be made by the methods of the previous section. However, the value of η_n to be used still requires satisfactory numbers for the quantities x_1 to x_4 of Equation (23). This was achieved with the aid of a computer optimization technique based on a method by Dickenson[7] which minimized the sum of the squared difference between calculation and measurement.

The limitations on computer storage space resulted in the decision to optimize in six different sets; one for each frequency on each radial. The values obtained were compatible for a given frequency, but not so between frequencies. The frequency differences varied smoothly across the band but were not constant as expected from the theoretical considerations. The differences were sufficiently large and significant to make a choice of compromise values for all frequencies in the 900 to 1500 kHz range impossible. The frequency difference obtained for the $f_1(B)$ (Equation (23)) value could be explained by a 'skin depth' phenomenon, i.e. the 'effective' conductivity is different at different frequencies as a result of differing penetration depths into an earth, whose conductivity varies with depth. A similar explanation may be found for the $f_2(B)$ difference but this is less clear at present.

A further possible reason for the discrepancy can be seen by examining Fig. 14 of the Appendix, (Section 10) which discusses the phenomenon, expected from theory, of a very low field strength at a critical range and for surface impedance close to a critical value. The sharply defined area with very low field will be less marked in practice due to fields being scattered from points other than those on the line between transmitter and receiver. In the optimization process a calculated field from such an area would be very different from the measurements and the optimization parameters would adjust to force the values away from this situation.

Except for the above problem the agreement between empricism and theory was satisfactory. The optimization gives f_1 and f_2 as functions of frequency:

$$f_1(B) = (1 - B)^{95/\lambda}$$
$$f_2(B) = \sqrt{\frac{\lambda B}{206}} - 1{\cdot}23B + 0{\cdot}35B^{1{\cdot}5} \qquad (33)$$

6. A working program

A computer program has been written* so that field strengths may be calculated for an operational purpose, i.e. to predict a service area. A flow chart of this program is given in Fig. 6 and an example of the output is shown in Fig. 7. This output gives the wavelength in metres, labelled as 'LAMBDA(M)'. The columns are as follows:

1. The distance of field point from transmitter in metres.
2. The terrain height in metres.
3. The average height assumed for buildings in metres.
4. The percentage of area covered by buildings.
5. The ground conductivity in millisiemens per metre.
6. and 7. Q_n as defined by Equation (24).
8. The magnitude of the loss relative to a perfectly conducting flat surface.
9. The phase of the loss factor.
10. Column 8 expressed as dB.
11. The electric field strength in millivolts per metre that is equivalent to the calculated magnetic field in a plane wave in free space.

This program was run to produce the fields which were described in Section 2. The results of these calculations are shown in Figs. 8 to 13. Each figure has the measurements plotted on it for comparison. It will be seen that the calculations closely follow the measurement features. The calculations for 908 kHz, Figs. 8 and 11, repeat the feature of high fields up to approximately 24 km from the transmitter. The steep decrease in field is well matched on each diagram as is the dip near the centre of London. This being the case even though these features differ dependent on frequency (compare Figs. 8, 9 and 10). Figs. 12 and 13 clearly show the repeated dip for the high buildings in the Croydon area. The standard deviations of the differences between calculations and measurements are as follows:

1. 1·9 dB for 908 kHz
2. 3 dB for 1214 kHz
3. 3·2 dB for 1457 kHz

7. Future work

Sufficient work has been done to demonstrate that the new calculation method is on the right lines. However, there is much more that could be done to fill in the finer details. Three points in particular require further investigation:

1. The ratio of the electric to magnetic field in the built-up area requires investigation. The theory indicates that the mean value of the electric field will be lower, relative to the magnetic field, than in rural areas.
2. The height gain to be expected requires confirmation by measurement.
3. The frequency dependence of the factors requires confirmation, in view of the discrepancy between the measurement and the theory offered.

* Much of the programming work was done by B. Tait.

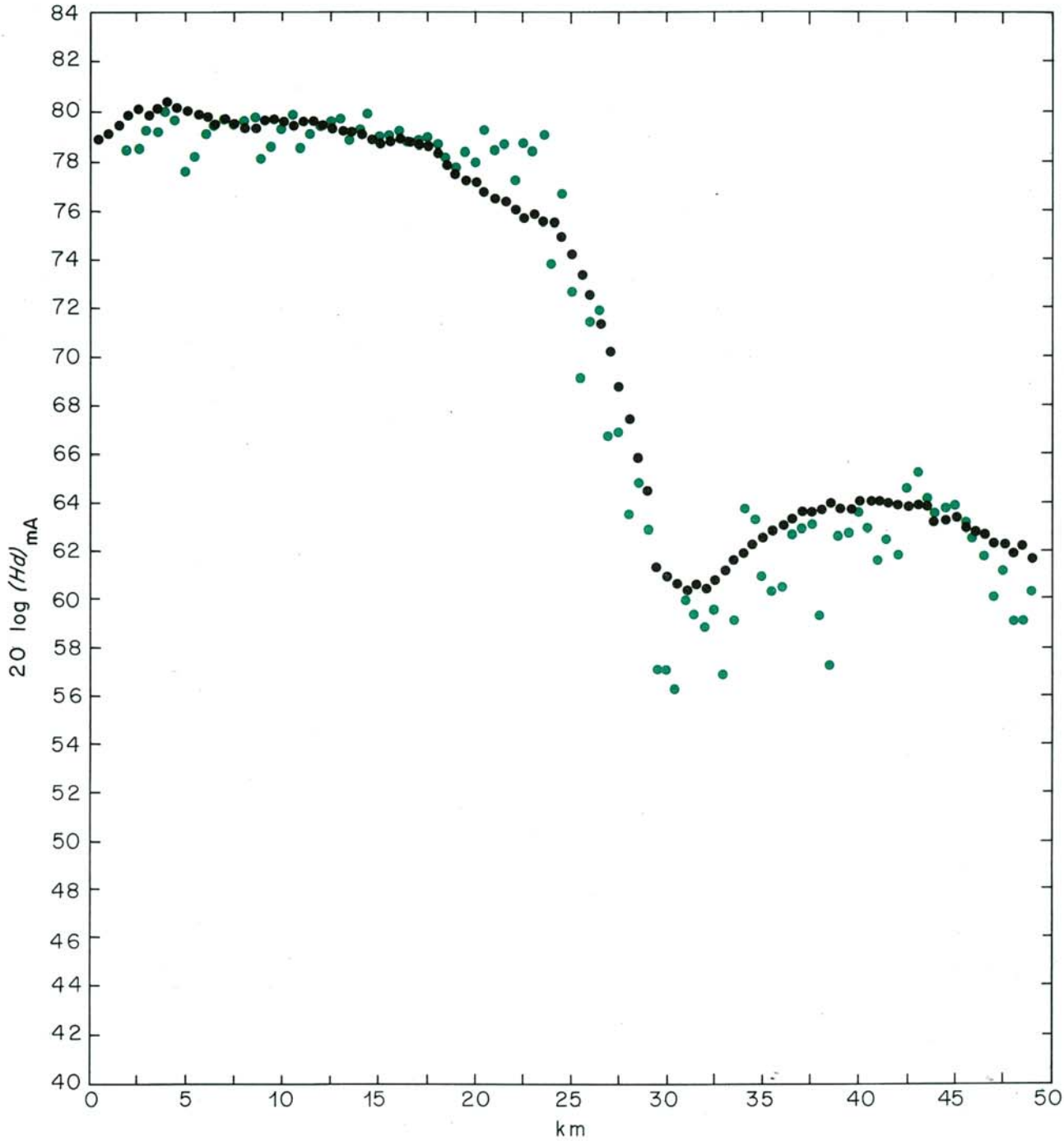

Fig. 8 - Results on the radial 181° E.G.N. at 908 kHz

● calculated ● measured

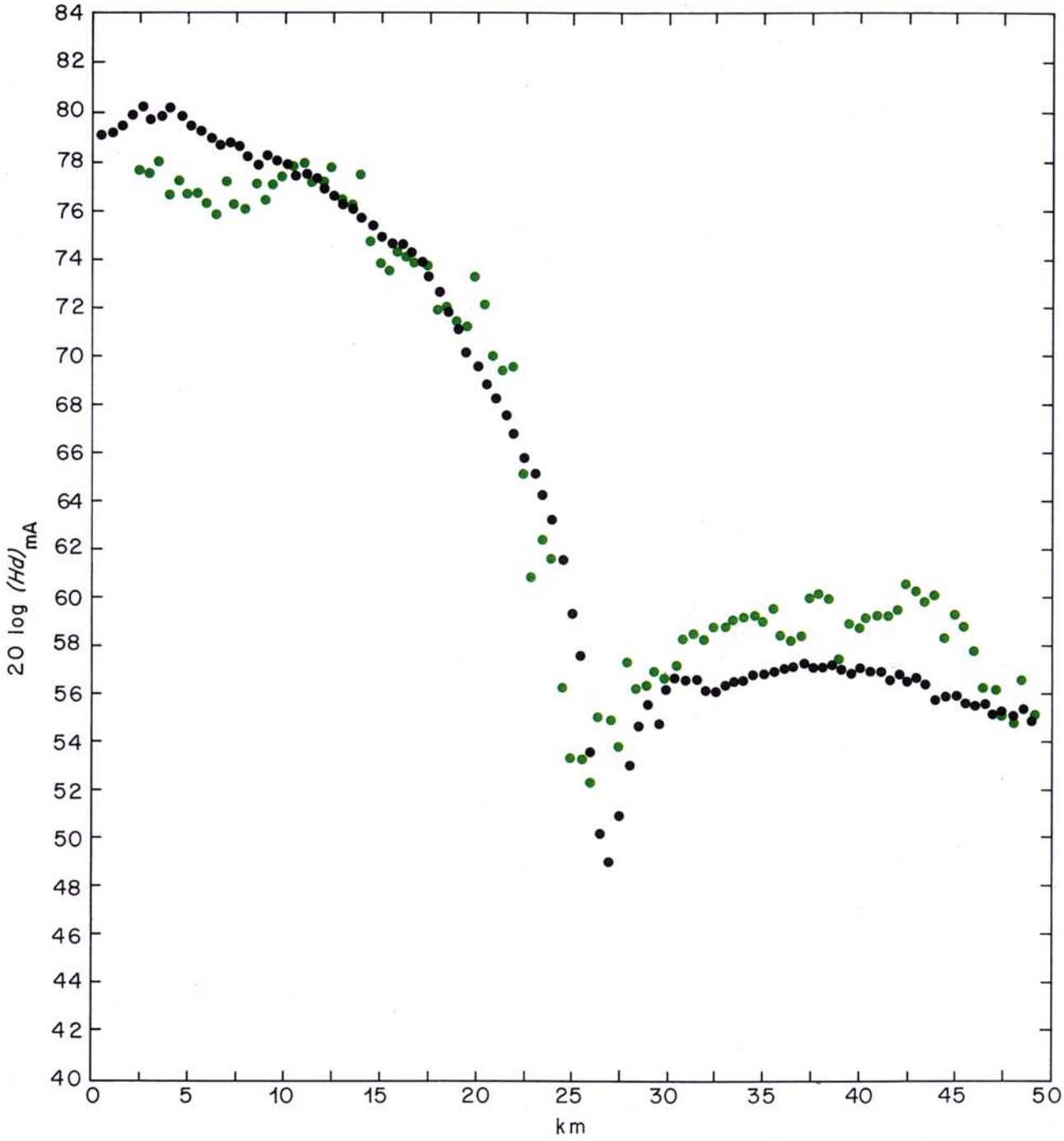

Fig. 9 - Results on the radial 181° E.G.N. at 1214 kHz

● calculated ● measured

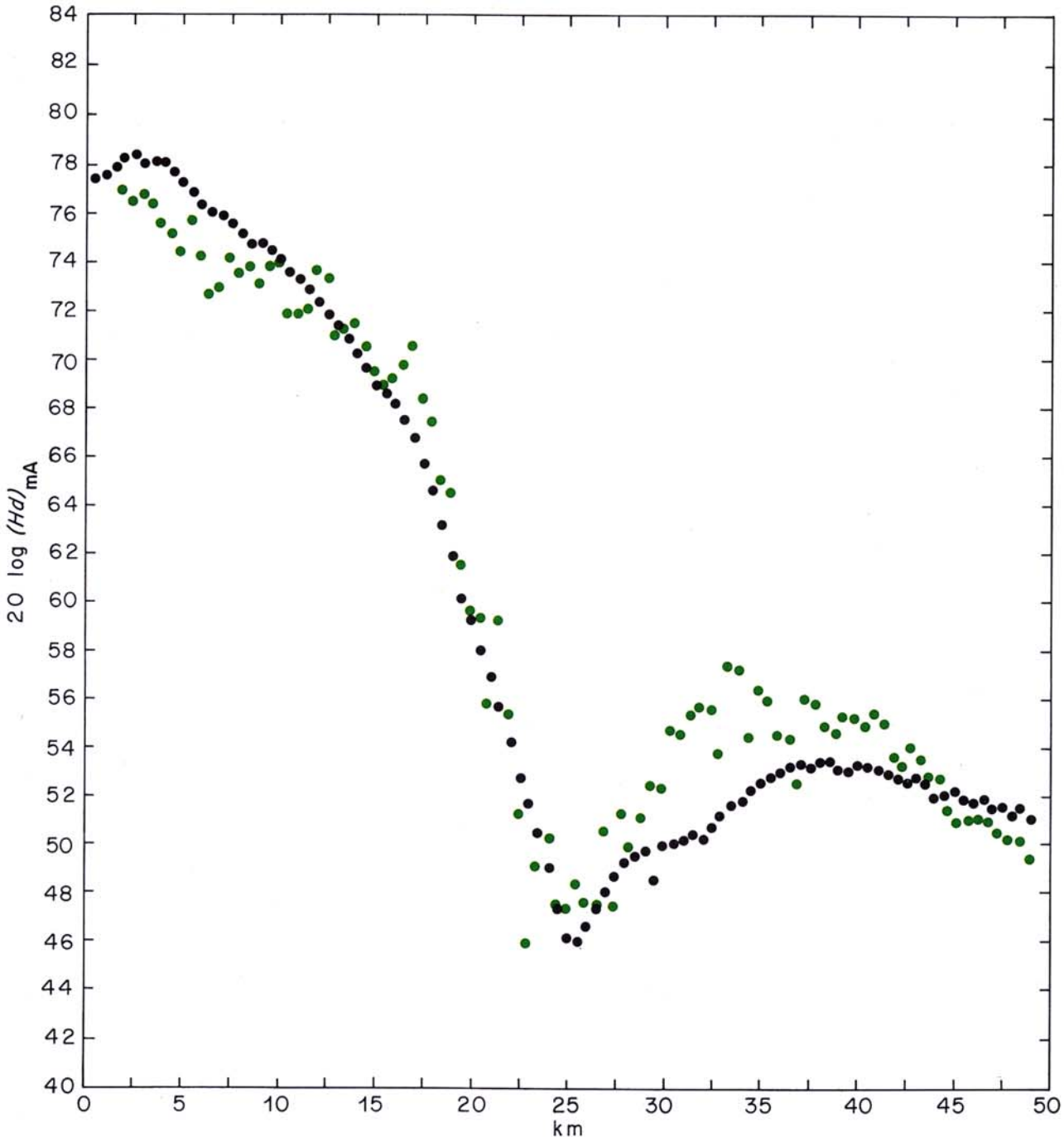

Fig. 10 - Results on the radial 181° E.G.N. at 1457 kHz

● calculated ● measured

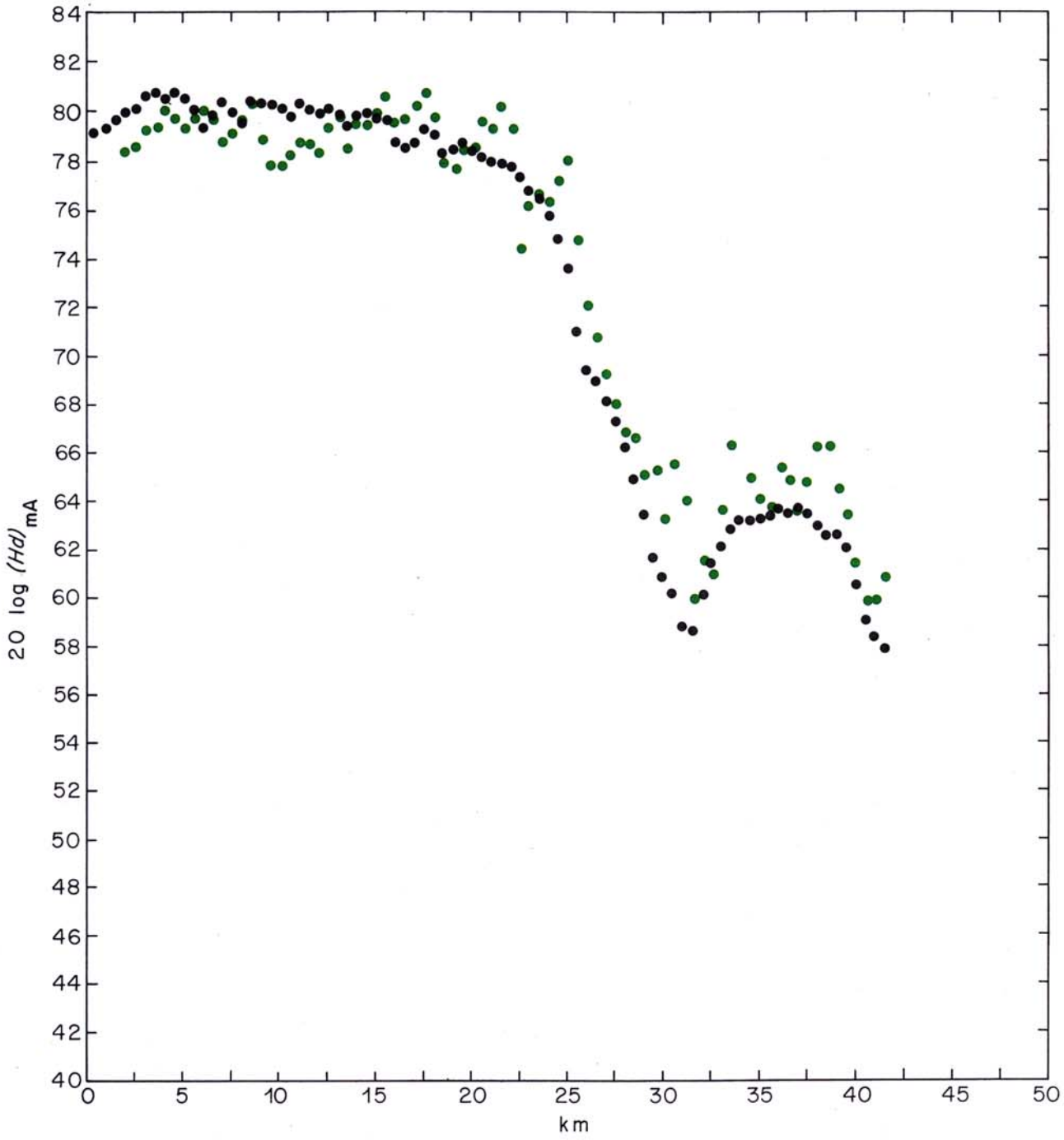

Fig. 11 - Results on the radial 169° E.G.N. at 908 kHz

● calculated ● measured

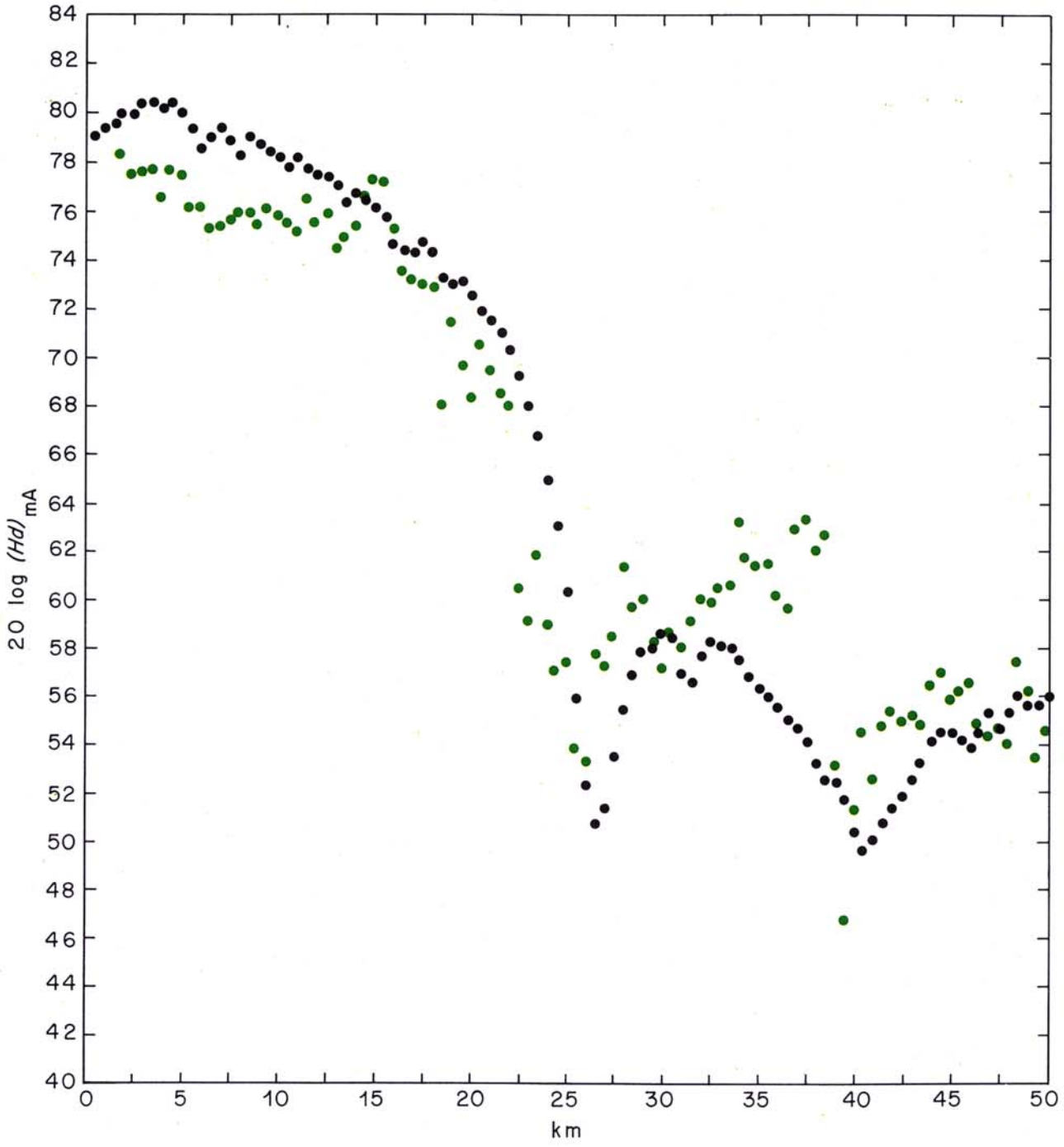

Fig. 12 - Results on the radial 169° E.G.N. at 1214 kHz

● calculated ● measured

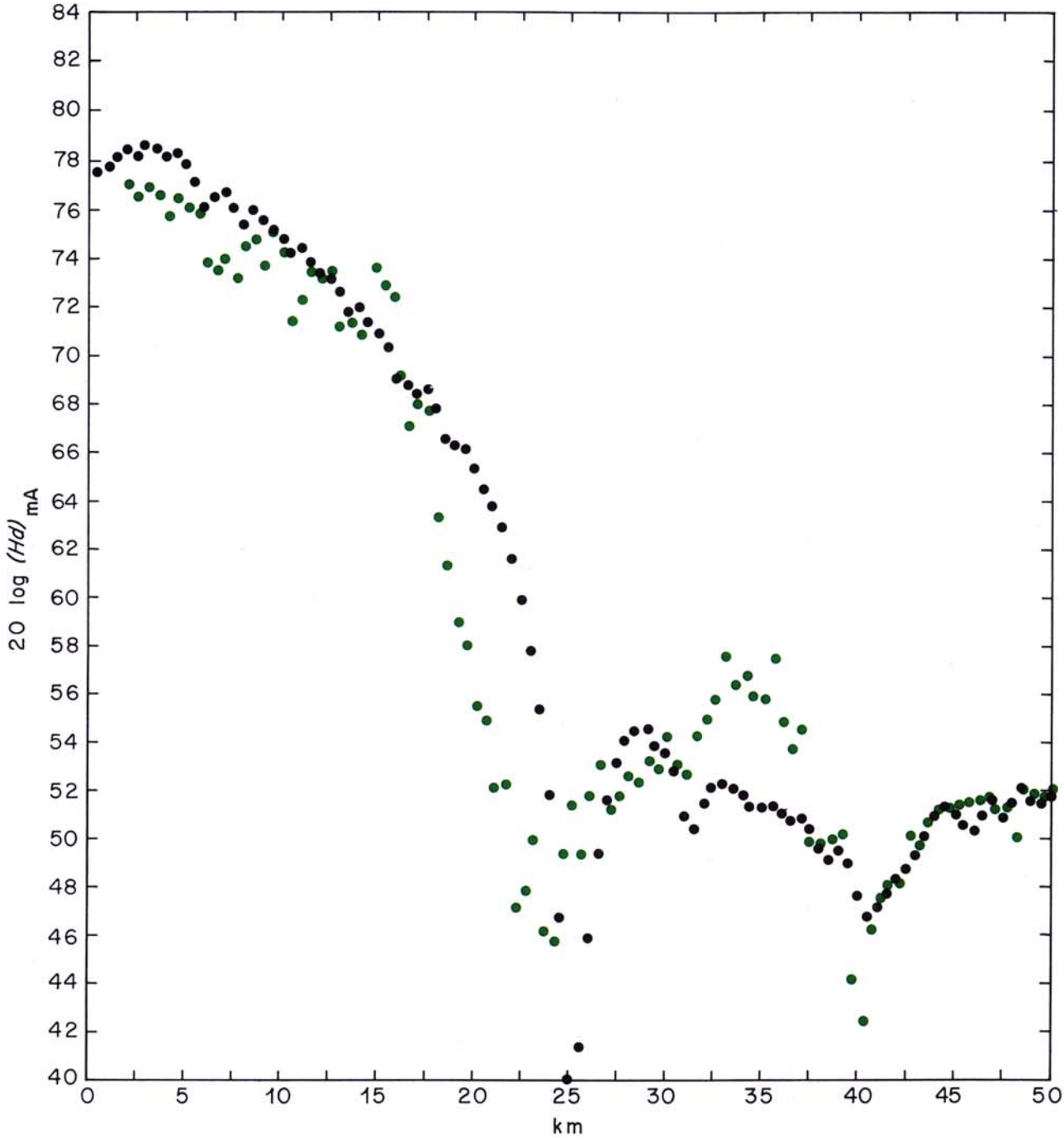

Fig. 13 - Results on the radial 169° E.G.N. at 1457 kHz

● calculated ● measured

There are certain features of the calculation method which could be improved. In particular a method could be devised to allow for off-axis scattering. This could simply take the form of a background field which would be a limit to how low the field would reduce in the difficult region shown in Fig. 14 and considered in the Appendix (Section 10).

The calculation system could be turned into a yet more economic tool for everyday planning. The data required can be extracted from banks such as those held for UHF planning.[8] The building data can be approximately inferred from the population data banks.[9]

It is probable that the methods employed here could be extended to other frequency bands, both higher and lower.

8. Conclusions

The problem of loss of medium-wave field strengths in towns has been considered for over 50 years, but no adequate prediction method has been developed. This report provides such a method, although further work is necessary to put it on a firmer basis and to turn it into a planning tool.

9. References

1. SUSANS, D.E., THODAY, R.D.C. *and* BUCKLEY, M.J. A medium-wave field-strength measuring receiver. BBC Research Department Report No. 1972/1.

2. JORDAN, E.C. 1950. Electro-magnetic waves and radiating systems. Constable and Co. Ltd.

3. ROWDEN, R.A. *and* BELL, C.P. 1975. The estimation of the service areas of medium- and long-wave broadcasting stations. BBC Research Department Report No. 1975/1.

4. MILLINGTON, G. 1948. Ground-wave propagation over an inhomogenous smooth earth. *Proceedings I.E.E.*, Part III, 1949, pp. 53 – 64.

5. HUFFORD, G.A. 1950. An integral equation approach to the problem of wave propagation over an irregular terrain. *Quart. J. Appl. Math.*, 1952, **9**, 4, pp. 391 – 404.

6. PAGE, H. 1963. An introduction to the theory of aerials. BBC Research Department Report No. E-085, Serial No. 1963/27.

7. DICKINSON, J.R. 1958. A computer program for system optimization. *Trans. Engineering Institute of Canada*, 1958, **2**, 4, pp. 157 – 161.

8. KING, R.W. *and* CAUSEBROOK, J.H. 1974. Computer programs for u.h.f. co-channel interference prediction using a terrain data bank. BBC Research Department Report No. 1974/6.

9. DAVIES, R.E. 1974. Population counts using a computer data bank. BBC Research Department Report No. 1974/14.

10. Appendix

The new calculation system proposed in this report is in a domain of the ground-wave phenomenon which is unfamiliar. It is therefore helpful to have a picture of the features to be expected in this domain. This led to the production of Fig. 14, where a set of contours is given of loss (dB) and phase (degrees) relative to free-space conditions for a wave travelling over homogeneous ground. These are drawn on the complex plane of ρ, the parameter defined by Equation (27) and on Fig. 14. This is a useful choice of parameter because profile lines are radials on this diagram, which can be seen from the definition of ρ. A practical profile cannot, in general, be determined from this diagram because it does not represent the situation where the surface impedance varies along the path.

The lower half of the figure represents the conventional domain and it will be seen that it is very regular and that the contours in it all represent loss relative to free space (negative dB's). The upper half represents the situation with buildings on the profile line and it will be seen that it contains a sharp irregularity and that radial lines can cross contours of enhanced field (positive dB's). The radial line making an angle of about 51° with the real axis passes through the deep zero singularity. Thus complex values of the surface impedance having angles of about 70·5° are critical. The calculations for this diagram were made with the formula of Equation (26) because this permits a simpler computation for the homogeneous profile. This makes the assumption that the mathematical form of Equation (26) has a physical reality in the positive quadrant of the parameter ρ. However, a check was made by obtaining some results from Equation (1). The agreement was very close; this gives reasonable justification for each of these equations because they have largely independent derivations. In addition, the extension into this new region produces field values that match the measured results thus producing a further justification.

A further understanding of Fig. 14 may be aided with an hypothetical example: let us take the case where un-

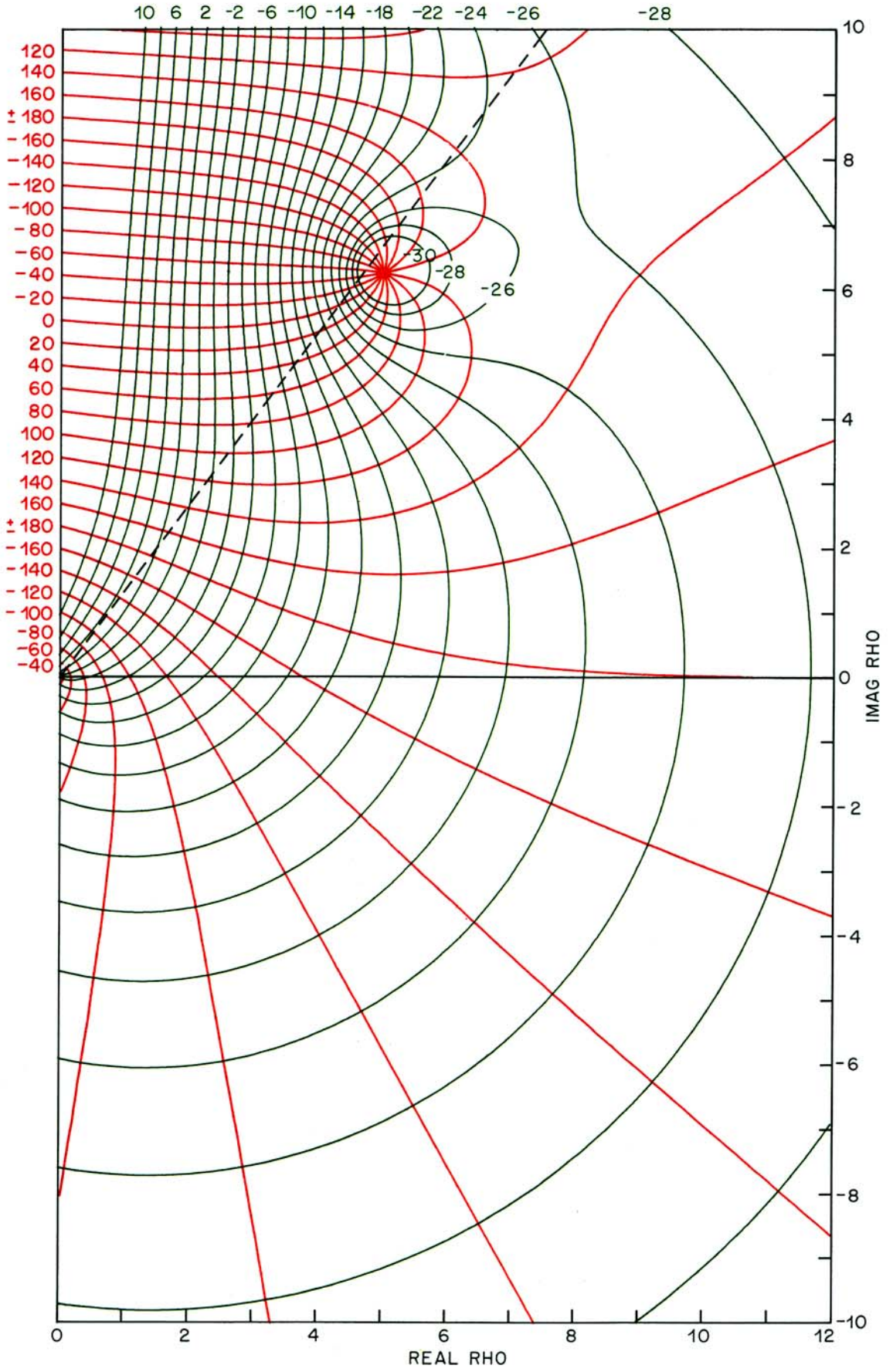

Fig. 14 - A mapping of the ground-wave attenuation on an Argand diagram of the parameter $\rho = -j\pi\eta^2 d/\lambda$

amplitude (dB rel. to free space) phase (deg. rel. to free space)

cluttered ground would give an $\eta = 0{\cdot}05 + j0{\cdot}05$ and assume it is evenly built-up along the whole profile, adding j0·1 to give:

$$\eta = 0{\cdot}05 + j0{\cdot}15 \qquad (34)$$

This results in a phase of 53·13 degrees for ρ which can be represented by the dotted black line on Fig. 14.

Then:

$$d/\lambda = 12{\cdot}7|\rho| \qquad (35)$$

The example results in the attenuation factor varying as shown in Fig. 15. This is very similar to the measured field variations (of Section 2 in the body of the report), even though the varying density of clutter is not included.

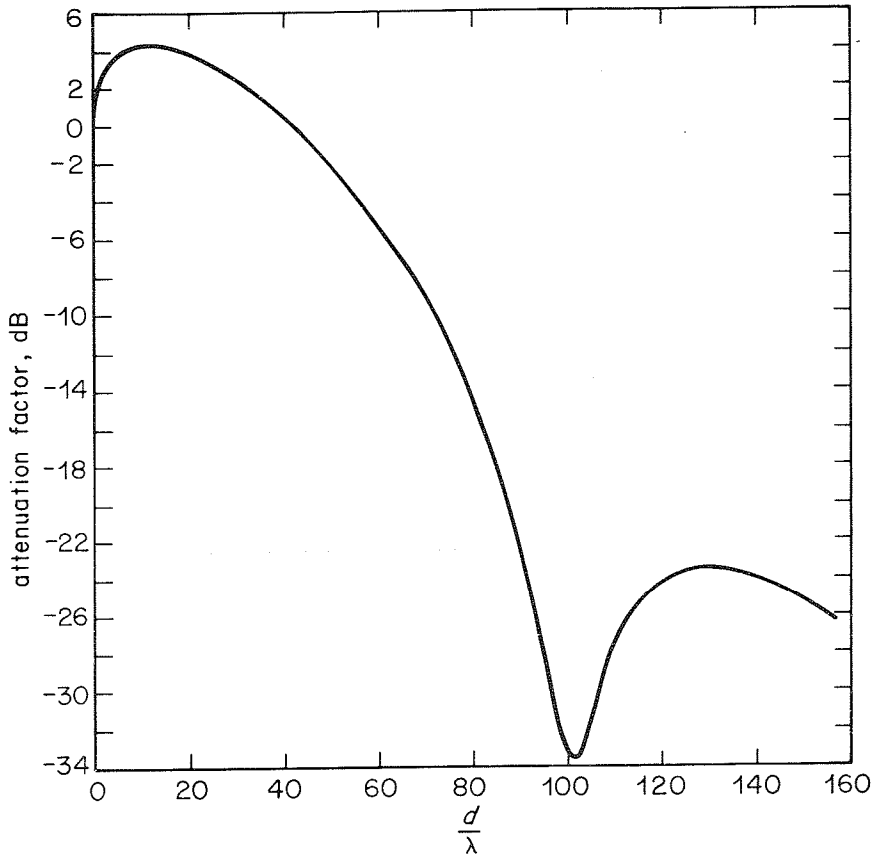

Fig. 15 - An hypothetical profile, assuming homogeneous ground and buildings